

Experimental Analysis of a Swirl Atomizer for High Differential Pressure

Roop Lal¹, Gaurav Luthra¹, R. C. Singh^{1*}, J. Singh¹, K. Khanna¹, Suresh Lal²,

¹Department of Mechanical Engineering, Delhi Technological University, Delhi 110042, India

²Center for Fire, Explosive and Environment Safety, Timarpur, Delhi 110007, India

*Email: rcsingh68@hotmail.com

Abstract: Researchers and scientist are continuously working on developing system for atomizing spray of minimum diameter droplets used for fire extinguisher and different fields of application in scientific life. In this research, a high pressure swirl atomizer was developed for performing at $8 \times 10^6 \text{ N/m}^2$. The spray characteristics of the designed and fabricated nozzle were experimentally evaluated. At the inlet of the nozzle the variation of the liquid supply pressure was considered in a range of 40 to 100 bar using laser diffraction techniques to achieve the optimum value of Sauter Mean Diameter (SMD) of 50 - 60 μm . The experimental observations of SMD were compared with the analytical model developed by Wang and Lefebvre (1987). It was observed that the spray cone angle was decreasing with the increase in pressure and the coefficient of discharge was nearly 0.65 through nozzle.

Keywords : Nozzle; High pressure swirl atomizer; Sauter mean diameter (SMD); Discharge coefficient; Spray cone angle

Nomenclature:

ρ = density of water, kg/m^3
 ρ_a = density of air, kg/m^3
 σ = surface tension of water, kg/s^2
 \dot{m}_L = liquid mass flow rate, kg/s
 A_a = air core area, m^2
 A_o = area of exit orifice, m^2
 A_p = area of inlet passage, m^2
 D_o = swirl chamber port area, m^2
 D_s = swirl chamber diameter, m
 D_o = liquid orifice diameter, m
 D_p = diameter of inlet passage, m
 L_p = length of inlet passage, m
 Re_{out} = Reynolds number at the exit orifice.
 We = Weber number
 $X = A_a/A_o$

i = number of inlet ports
 K = Atomizer geometric constant
 θ = spray cone half angle, deg
 C_D = discharge coefficient
 U_o = exit velocity of liquid, m/s
 μ = dynamic viscosity, m^2/s
 ν = kinematic viscosity, kg/ms
 ρ = density, kg/m^3
 σ = surface tension, kg/s^2
 ΔP = Differential Pressure, bar
 t = thickness of liquid sheet, mm
 SMD = Sauter Mean Diameter, μm

Subscript:

_L = liquid phase
_O = orifice

I. INTRODUCTION

A series of research and development over the years in the field of pressure swirl atomizers has led to its use in several industries like agriculture, chemical, fuel injected engines, fire suppression system, etc. The major advantage of this type of atomizer is its versatility to produce small liquid droplets at a wide range of pressure. They are preferred due to their simple design, ease of manufacturing and good spray characteristics.

In the pressure swirl atomizer, the liquid enters the swirl chamber through number of tangential passages imparting an

angular velocity to the liquid. Inside the nozzle, the liquid possess axial as well as tangential velocity leading to the formation of helical flow in the swirl chamber. Due to the swirling motion, centrifugal forces act upon the liquid and an air core vortex is formed at the centre. So, when the liquid exits the nozzle, a thin sheet of liquid is formed at the exit orifice. These thin sheets of liquid are then subjected to surface instability due to combined effect of its high velocity, surface tension forces and drag forces of the surrounding air as the liquid leaves the exit orifice. These surface protuberances further convert into unstable ligaments which finally disintegrate into smaller droplets.

Figure 1 shows the schematic of a pressure swirl atomizer. The tangential passages leading to swirl chamber, the air vortex and thin liquid sheet are shown.

According to Taylor (1948) [1] and Giffen and Muraszew's (1953) [2] principle of maximum flow, discharge coefficient C_D expressed as a function of X , is a maximum, or $1/C_D^2$ is a minimum.

$$1/C_D^2 = 1/K^2 X + 1/(1-X)^2 \quad \text{-----(1)}$$

Differentiating $1/C_D^2$ with respect to x and equating to zero, $2K^2 X^2 = (1-X)^3$

Based on the assumption of inviscid flow and features of internal flow are ignored. But recent studies (Yule et al. 1997 [3], Holtzclaw et al. 1997 [4]) show that the performance parameters depend not only on nozzle geometry but also on internal flow features as shown in fig.1..

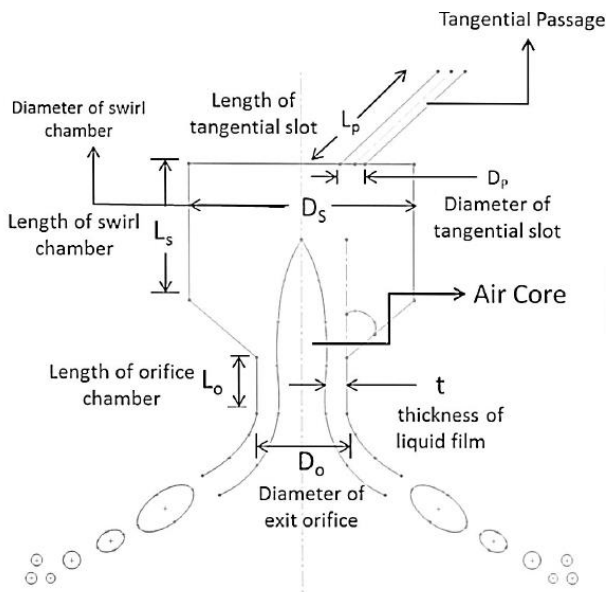


Figure 1. Schematic of Pressure swirl atomizer

An elaborate study has been done by Wang and Lefebvre [5] on mean droplet size of the particle. They studied the effect of forces such as inertial forces, aerodynamics forces and surface tension forces on the droplet size. An empirical correlation of Sauter Mean Diameter with the properties of the liquid, pressure applied and the spray characteristics of the nozzle were derived by conducting experiments on six different nozzles by them.

The basic understanding of the spray characteristics of a simplex nozzle was achieved by development of various theoretical models on film thickness, spray angle and discharge coefficient by Dombrowski and Johns [6], Dombrowski and Hassan [7], Clark and Dombrowski [8], Rizk and Lefebvre [9], Suyari and Lefebvre [10] and Yule and Chinn [11]

The philosophy here has been to take an existing design, which operates reasonably satisfactorily at high pressure, and to use this as a benchmark, or starting point, for the subsequent testing of variations of geometry and dimensions.

Work by Carlisle and Radcliffe [12] and Risk and Lefebvre relating C_D with various geometric parameters like D_s , A_p and D_o are important with respect to designing of the atomizer. The swirl atomizer can be used in I. C. Engine [16,

17] for the proper combustion and producing high pressure in combustion chamber.

1.1 Geometrical parameters of the atomizer

The following geometrical and dimensionless parameter governs the design of an atomizer. $A_p/(D_s.D_o)$, D_s/D_o , L_s/D_s , L_o/D_o and L_p/D_p where D_o is a chosen parameter.

With increase in the geometry ratio L_s/D_s , C_D and t increases, however spray cone angle decreases. Thus it should be under optimal extreme values. Recommended value is 0.7 for most of the cases where the pressure drop is constant. This has been studied and established by J. Xue et al [13] in their research. The other geometrical parameter L_o/D_o behave unlike L_s/D_s . With increase in L_o/D_o , C_D , t and spray cone angles decreases sharply and then increases slightly thus it should be reduced to minimum value. L_p/D_p as stated by Tipler and Wilson [14] in their research must not be less than 1.3 to avoid unstable spray.

The thickness of the film 't' reduces with the increase in D_s/D_o when K , i.e. $A_p/(D_s.D_o)$ is kept constant. Discharge coefficient and spray cone angle decreases with increase in D_s/D_o .

The geometrical parameters can be determine depending on the C_D that can be known by eq. (1)

$$C_D = m_L/[A_o(2\rho.\Delta P)^{1/2}]$$

A_o is a constant due to chosen value of D_o which is 1 mm.

Results obtained by Carlisle [3] and Risk and Lefebvre [4] given by equations (2) and (3) respectively were two other relations for C_D and geometrical parameters. These equations were used to find the ratios, D_s/D_o and $A_p/(D_s.D_o)$.

$$C_D = [0.0616 (D_s/D_o)\{A_p/(D_s.D_o)\}]^{1/2} \quad (2)$$

$$C_D = 0.35 (D_s/D_o)^{0.25} [A_p/(D_s.D_o)]^{0.5} \quad (3)$$

Taylor's inviscid theory showed the simplicity in calculating spray cone angle which is solely dependent on swirl chamber geometry and the geometric constant, K , as given in eq. (4) below.

$$\sin(\theta) = \pi/2 (1-X)^{1.5} / K (1-\sqrt{X})(1+X)^{0.5} \quad (4)$$

where K is $A_p/(D_s.D_o)$. To realize the value for spray cone angle, the values of $K=A_p/(D_s.D_o)$ and X is used in the relation (4) with X derived from equation (5), as stated by Giffen and Muraszew.

$$C_D = 1.17 [(1-X^3)/(1+X)]^{0.5} \quad (5)$$

Thickness of the liquid sheet 't' is then ascertained with the help of X .

$$\text{Where, } X = (D_o - 2t)^2 / (D_o)^2 \quad (6)$$

The Sauter Mean Diameter (SMD) is then calculated with the help of equation (7) given by Wang and Lefebvre,

$$\text{SMD} = 4.52 (\sigma\mu^2 / \rho_a \Delta P_L^2)^{0.25} (t \cos\theta)^{0.25} + 0.39 (\sigma\rho_L / \rho_a \Delta P)^{0.25} (t \cos\theta)^{0.75} \quad (7)$$

where values for θ and t were used from equation (4) and equation (6) respectively

Table 1. Given parameters for the designing of the atomizer

Properties	Value
$\rho_L(\text{kg.m}^{-3})$	1.0×10^3
$\rho_a(\text{kg.m}^{-3})$	1.0

$\mu_L(\text{kg.s}^{-2})$	1.0×10^{-03}
$D_o(\text{m})$	1.0×10^{-03}
$\sigma(\text{kg.s}^{-2})$	7.34×10^{-02}
$\dot{m}_L(\text{kg.s}^{-1})$	6.5×10^{-021}
$\Delta P_L(\text{MPa})$	8.0

II. EXPERIMENTAL SETUP:

A high pressure pump of a pumping limit of 100 bar was used to introduce water into the atomizer controlled by a flow meter and a control valve fig. 2. The pressure was varied from 40 to 100 bar using a bypass valve and controlling the rpm of the pump, simultaneously. The actual mass flow rate through the nozzle was measured at different pressures with an increment of 10 bar. Water was collected into the reservoir having a vertical scale for duration of 1 minute at different pressures. At these pressures, spray cone angles were also measured using an angular scale.

A particle size analyzer (Insitac/Malvern) based on laser scattering technology was used to measure the average particle diameter of the spray formed by the nozzle. The exit of the nozzle was placed at a vertical height of 1 m from the instrument. The dynamic measurement range for this system for this system was between 0.1 to 2500 μm . It uses 5mW/670 nm diode laser with a beam diameter of 10 mm. The accuracy of the instrument was $\pm 2\%$ on Dv(50) reported using the verification reticle (specified by the manufacturer). It could measure the size distribution of sprays with obscurations up to 95%. The measurement rate of equipment was one measurement 68 every 400 μs . The operating principle of the instrument is based on Mie theory of light-particle interaction to obtain the particle size distribution. The photodetector sends a signal to the computer program (RTSizer, Insitac/Malvern) generated from the scattered light. It then display the values of SMD, Dv(10), Dv(50), Dv(90) and the particle size distribution on the screen

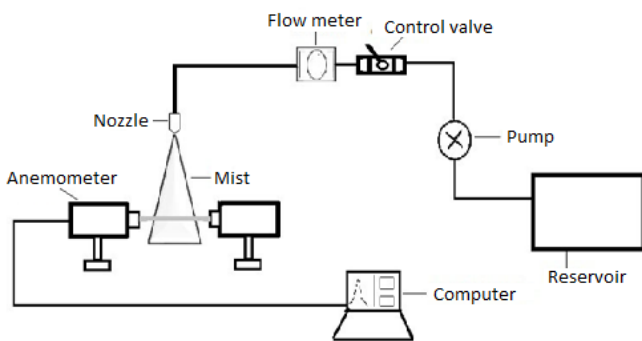


Figure 2. Experimental setup

III. RESULTS AND DISCUSSION

Table 2 gives the calculated result of the geometrical parameters and spray characteristics of atomizer. Fig. 3 and fig. 4 shows the Solid Works model of the atomizer.

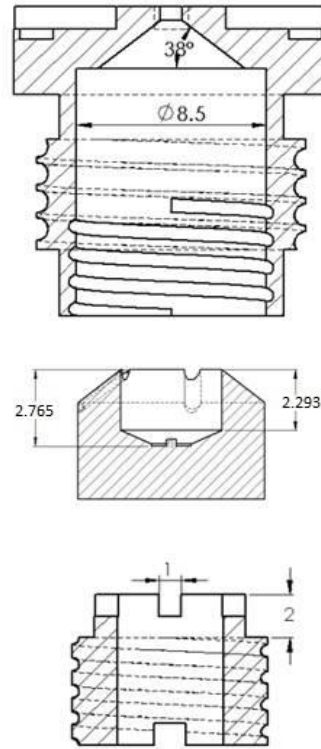


Figure 3. Cross section of the atomizer

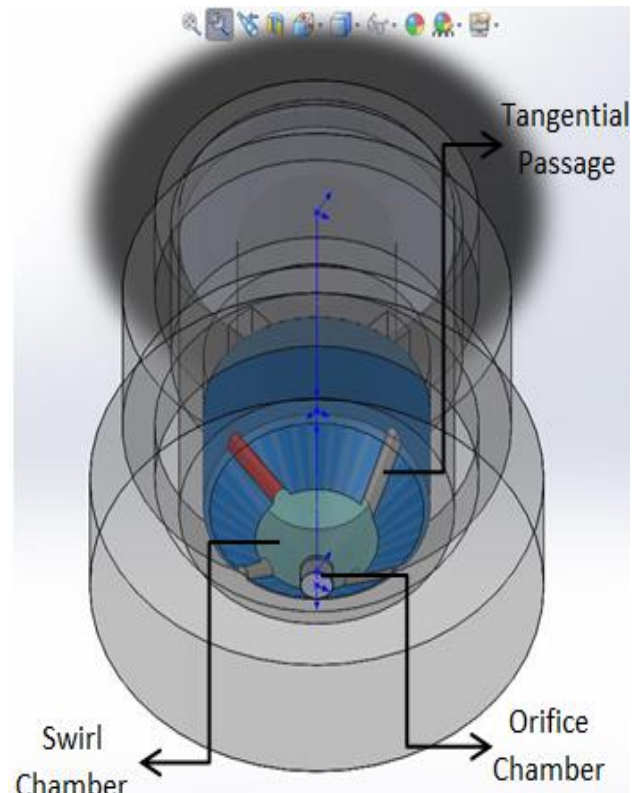


Figure 4. Solid Works 3D model of the atomizer

Table 2 Final Result from the designed atomizer

A_p	1.605 mm^2	C_D	0.654
-------	----------------------	-------	-------

i	4	K	0.406
D_s	3.95 mm^2	θ	31.26°
L_s	2.765 mm^2	t	0.242 mm
L_o	0.5 mm^2	X	0.267
U_o	82.80 m.s^{-1}	SMD	$67.89 \mu\text{m}$

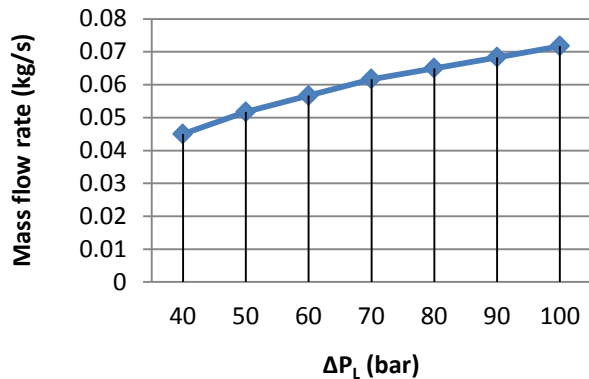


Figure 5a. Experimental mass flow rate Vs pressure difference

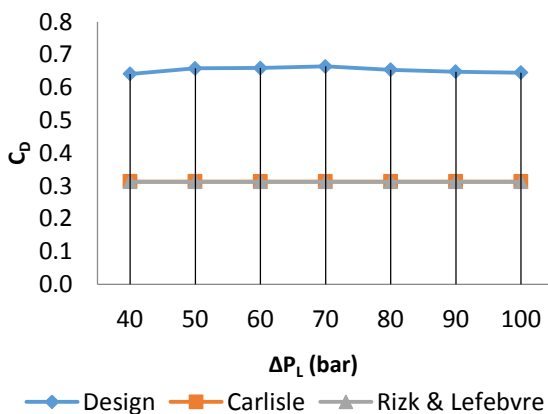


Figure 5 b. Experimental discharge coefficient Vs pressure difference

Fig. 5a shows the liquid mass flow rate and 5b represent the discharge coefficient as a function of liquid supply pressure. C_D doesn't vary much with ΔP_L and has a range of $0.640 < C_D < 0.6645$ with $C_{D \text{ max.}} = 0.6645$ at 70 bar. The curve seems to comply with the principle of maximum flow given by Giffen and Muraszew [2] as discussed in section 1. The air core formed inside the nozzle adjusts itself with change in pressure applied, to give a maximum liquid flow rate though the nozzle at all pressures. Fig. 5b also shows the C_D estimated according to the models developed by Carlisle and Risk & Lefebvre [8, 9]. These curves are a straight line parallel to the x-axis but offset from the experimental C_D . The value of half spray cone angle at design point ($\Delta P_L = 80$ bar) was found to be 31.09° as compared to the experimental value of 34° . The cone angle of a spray is a characteristic of an atomizer which basically depends on the swirl chamber geometry and is in inverse relation with K as predicted by

Taylor [1]. According to Datta and Som [15], with an increase in the flow rate Q, at its lower range, there occurs a sharp increase in the spray cone angle, however θ becomes almost independent of the flow rate Q or ΔP_L at its higher range. From our experimental findings, spray cone angle θ decreases slightly from 39° to 31° over the range.

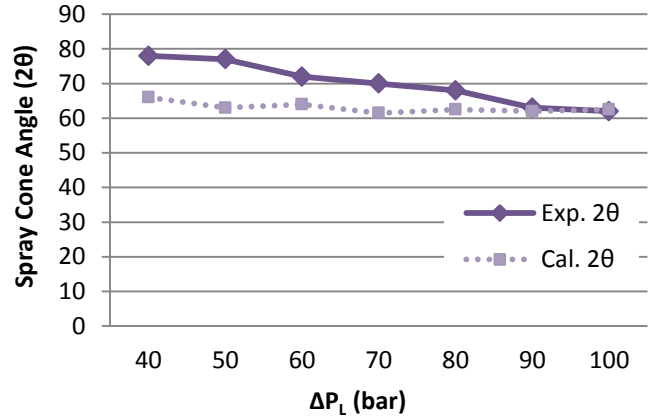


Figure 6. Variation of spray cone angle (2θ) with varying ΔP_L

Fig. 6 shows a variation of spray cone angle with ΔP_L . The reason behind the decreasing trend may be due to the ejector action of the high velocity spray that generates air currents, which cause the spray angle to contract. This effect is aggravated by the increase in spray velocity that accompanies an increase in ΔP_L . Fig. 6 also shows the theoretical results derived from eq. (4). Over a pressure range of $40 < P_L < 80$ bar, both the curves show a similar trend, moreover, the values of the experimental and the theoretical findings are quite close to each other. Besides this, the two curves meet each other over the 90 to 100 bar range having an approximate value of 31° .

Fig. 7 shows a graph between the experimental and theoretical values of the Sauter mean diameter of the particles. The theoretical values have been obtained from eq. (7) given by Wang and Lefebvre [3]. From the graph it can be observed that for $\Delta P_L > 60$ bar the slope of the two curves get approximately same, tracing a similar decreasing trend. Although an initial relative large difference between the two curves becomes less and gets cone angle of a spray is a characteristic of an nozzle.

At lower pressure range, the frictional resistance from the swirl chamber walls decreases the turbulence, thereby, increasing the value of experimentally found SMD, whereas, an increase in pressure is accompanied by an increase in swirling strength while decreasing the subsequent decay due to frictional effect in the nozzle. Therefore, at high pressure, frictional effect becomes negligible and the difference between the two curves becomes constant, thus validating the Wang and Lefebvre's [3] model in this pressure range.

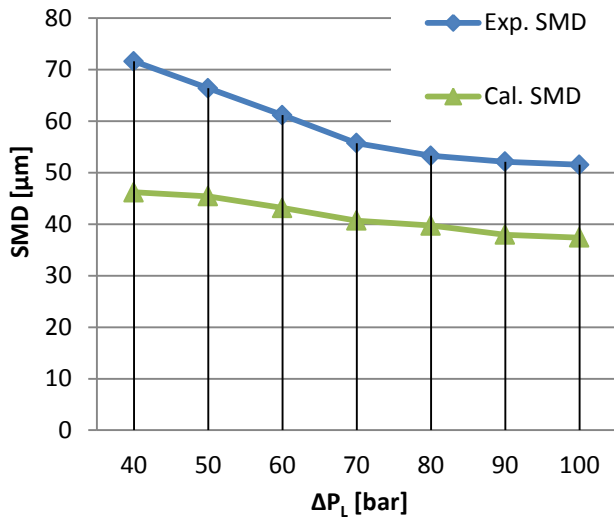


Figure 7. Variation of SMD with ΔP_L

IV. CONCLUSIONS

The designed and fabricated high pressure swirl atomizer delivered high mass flow rates and optimum spray characteristics.

i) The experimental measured SMD curve has a decreasing trend with increase in pressure from 40 to 100 bar but had a greater value compared to the values derived from Wang and Lefebvre empirical relation.

ii) The coefficient of discharge was nearly 0.65 throughout the working pressure range due to the air core adjusting itself to provide maximum flow rate.

iii) The spray cone angle decreases with the increasing pressure from 78 to 62.5 which was also confirmed by the theoretical data.

ACKNOWLEDGEMENT

The authors are thankful to Center for Fire, Explosive and Environment Safety, DRDO, Delhi for providing their experimental support

REFERENCES

[1] G.I. Taylor (1948). The Mechanics of a swirl atomizers. *7th international congress for Applied Mechanics* 2(1), 280-285.
 [2] E. Giffen and A. Muraszew, *The atomisation of liquid fuel* (Chapman and Hall, London, 1953).
 [3] A. J. Yule and J. J.Chinn (1997). Pressure Swirl Atomizer Internal Flow and Performance. *10th Annual Conference on Liquid and Spray Systems, Ottawa, Ontario, 90-94.*

[4] D.Holtzclaw, T. Sakman, S. M. Jeng, M.A. Jog and M Benjamin (1997). Investigation of Flow in a Simplex Fuel Nozzle *AIAA Paper No. 97-2970, 33rd AIAA/ASME/SAE/ASEE Joint Propulsion Conference & Exhibit, Seattle, WA.*
 [5] X. F. Wang and A. H. Lefebvre (1987). Mean Droplet Size from Pressure - Swirl Nozzles. *AIAA J. Propulsion Power, 3(1), 11-18.*
 [6] N. Dombrowski, W.R. Johns (1963). The aerodynamic instability and disintegration of viscous liquid sheets. *Chem. Eng. Sci. 18, 203-214.*
 [7] N. Dombrowski, D. Hassan (1969). The flow characteristics of swirl centrifugal spray pressure nozzles with low viscosity liquids. *AIChEJ. 15, 404.*
 [8] C.J. Clark, N. Dombrowski (1972). Aerodynamic instability and disintegration of inviscid liquid sheets. *Proc. Roy. Soc. London Ser. A Math. Phys. Sci. 329, 467-478.*
 [9] Risk N K and Lefebvre A H (1985). Internal Flow Characteristics of Simplex Swirl Atomizers. *Journal of Propulsion Power, Vol. 1, No. 3, 193-199.*
 [10] M. Suyari, A.H. Lefebvre (1986). Film thickness measurements in a simplex swirl atomizer. *J. Propul. 2 528-533.*
 [11] A.J. Yule, J.J. Chinn (1994). Swirl Atomizer Flow: classical inviscid theory revisited: *Sixth International Conference on Liquid Atomization and Spray Systems, Rouen, France, 334-34, 1.*
 [12] A. Radcliffe and D. R. Carlisle (1955). Communication on the Performance of a Type of Swirl Atomizer. *Proc. Inst. Mech. Eng., Vol. 169, p.101.*
 [13] J. Xue, M. A. Jog, S. M. Jeng, E. Steinthorsson, M. A. Benjamin (2002). Influence of Geometry on the Performance of Simplex Nozzles under Constant Pressure drop. *15th Annual Conference on Liquid Atomization and Spray Systems.*
 [14] W Tipler and A W Wilson (1959). Combustion in Gas Turbines. *Proceedings of the Congress International des Machines a Combustion (CIMAC), Paris, 897 - 927.*
 [15] A. Datta, S.K. Som (2000). Numerical prediction of air core diameter coefficient of discharge and spray cone angle of a swirl spray pressure nozzle. *International Journal of Heat and Fluid Flow, 21 412-419.*
 [16] R C Singh, R Chaudhary, R K Pandey and S Maji (2012). Experimental studies for the role of piston rings' face profiles on performance of a diesel engine fueled with diesel and jatropa based biodiesel. *Journal of Scientific & Industrial Research, Vol. 71, 57-62.*
 [17] R. C. Singh, R. K. Pandey, S. Maji (2016). An Overview-Tribological Aspects at the Interface of Piston Ring and Cylinder Liner for Improving the Performance of IC Engine. *International journal of advanced production and industrial engineering, Vol 1(1), 11-13.*
 [18] Ranganath. M. S, R. C. Singh, Rajiv Chaudhary, R. K. Pandey, (2014) Experimental Investigation of Friction and Wear Behavior at the Interface of Aluminium and Mild Steel, *International journal of advanced Research and Innovation, Vol 2(4), 775-780*
 [19] R C Singh, R K Pandey, Rooplal, Ranganath M. S, S Maji, (2016) Tribological performance analysis of textured steel surfaces underlubricating conditions, *IOP Publishing, Surf. Topogr.: Metrol. Prop.4/3, 034005*